JACS
JOURNAL OF THE AMERICAN CHEMICAL SOCIETY
Article
pubs.acs.org/JACS

Introducing Copper as Catalyst for Oxidative Alkane Dehydrogenation

Ana Conde,[‡] Laia Vilella,[†] David Balcells,*[,†,§] M. Mar Díaz-Requejo,*[,‡] Agustí Lledós,*[,†] and Pedro J. Pérez*[,‡]

[‡]Laboratorio de Catálisis Homogénea, Departamento de Química y Ciencia de los Materiales, Unidad Asociada al CSIC, CIQSO-Centro de Investigación en Química Sostenible, Universidad de Huelva, Campus de El Carmen 21007 Huelva, Spain

[†]Departament de Química, Universitat Autònoma de Barcelona, 08193 Bellaterra, Spain

[§]Centre for Theoretical and Computational Chemistry, Department of Chemistry, University of Oslo, P.O. Box 1033, Blindern N-0315, Oslo, Norway

Supporting Information

ABSTRACT: The dehydrogenation of *n*-hexane and cycloalkanes giving *n*-hexene and cycloalkenes has been observed in the reaction of such hydrocarbons with hydrogen peroxide, in the presence of copper complexes bearing trispyrazolylborate ligands. This catalytic transformation provides the typical oxidation products (alcohol and ketones) with small amounts of the alkenes, a novel feature in this kind of oxidative processes. Experimental data exclude the participation of hydroxyl radicals derived from Fenton-like reaction mechanisms. DFT studies support a copper-oxo active species, which initiates the reaction by H abstraction. Spin crossover from the triplet to the singlet state, which is required to recover the catalyst, yields the major hydroxylation and minor dehydrogenation products. Further calculations suggested that the superoxo and hydroperoxo species are less reactive than the oxo. A complete mechanistic proposal in agreement with all experimental and computational data is proposed.

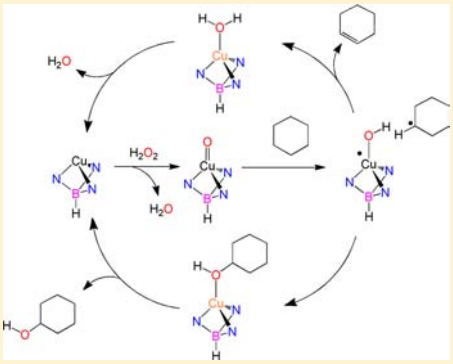

INTRODUCTION

The catalytic dehydrogenation of alkanes is probably one of the emerging areas in both organometallic chemistry and homogeneous catalysis that might have a tremendous impact in chemical industry in the next decades, due to the increasing use of olefins as raw materials.[1] The availability of alkanes in terms of their abundance and low cost makes this reaction an attractive route toward olefins. Usually this reaction (eq 1)

$$R^1\text{-}CH_2\text{-}CH_2\text{-}R^2 + SA \longrightarrow R^1\text{-}CH{=}CH\text{-}R^2 + SAH_2 \quad (1)$$

SA = sacrificial acceptor

requires the presence of a sacrificial hydrogen acceptor, another olefin in most cases.[1] At the industrial level, the dehydrogenation of alkanes is a known process that is based on the use of heterogeneous catalysts operating at high temperature (500−900 °C), with low control over selectivity.[2] In contrast, the homogeneous catalysts developed to date operate at a lower temperature (100−150 °C), allowing catalyst design toward control of the reaction outcome. Among the catalysts described to date, those based on iridium are the most active by far.[1] In nature, dehydrogenation is catalyzed by the desaturase oxidoreductase, which converts a C−C bond into the corresponding C═C bond, upon formal loss of two hydrogens.[3] Desaturases and hydroxylases reduce dioxygen to give the alkene or the alcohol, respectively (Scheme 1). Both

Scheme 1. The Desaturase and Hydroxylase Reactions with Dioxygen

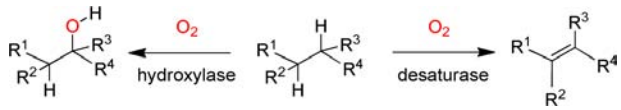

enzymes have been modeled at different degree, with only a few examples of transition metal complexes mimicking the desaturase function being described to date. Que and co-workers reported[4a] the stoichiometric reaction of a dinuclear iron-complex with cumene to yield α-methylstyrene as the result of the desaturation reaction (Scheme 2a), a work later expanded to several hydrocarbons.[4b,c] Crabtree, Eisenstein and co-workers first described[5] the catalytic use of a manganese-based system for the desaturation of dihydrophenanthrene with PhIO or oxone as the oxidant (Scheme 2b), in a transformation driven by the aromatization of the final products. Yin and co-workers later reported[6] the use of oxone to desaturate dihydroanthracene with other manganese-based catalysts (Scheme 2c). Shaik and Nam[8] have studied the interaction of iron(IV)-oxo species with such substrates, providing dehydrogenated compounds in substoichiometric amounts. In the

Received: November 4, 2012
Published: February 14, 2013

   dx.doi.org/10.1021/ja310866k | *J. Am. Chem. Soc.* 2013, 135, 3887−3896

Scheme 2. Model Systems for Desaturase

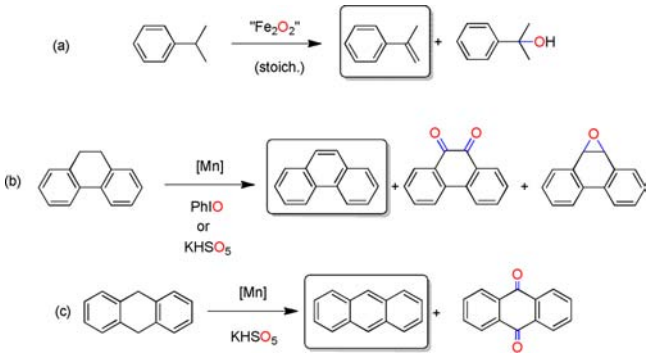

above catalytic cases, the reaction took place onto benzylic C–H bonds, a somewhat activated reaction site (bond dissociation energy of ca. 90 kcal/mol),[7] and additionally, in both manganese systems, desaturation led to aromatization. It is worth mentioning that this dehydrogenation process has not yet been described for nonactivated C–H bonds as those of cycloalkanes or lineal alkanes, with bond dissociation energies of 96–100 kcal/mol, respectively.[7]

We are currently interested in the development of catalysts for the direct oxidation of hydrocarbons, particularly methane or benzene into methanol and phenol respectively. This area constitutes a major goal in modern chemistry, since neither methanol nor phenol can be directly prepared in an efficient manner from the parent hydrocarbons. Methanol is prepared from syngas,[9a] whereas the manufacture of phenol takes place through the cumene process.[9b] We have recently described the catalytic potential of complexes of composition Tp^xCu (Tp^x = hydrotrispyrazolylborate[10] ligand, Scheme 3) for the direct

Scheme 3. Trispyrazolylborate Ligands

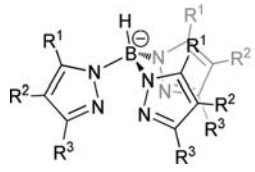

Tp^{Br3}: $R^1 = R^2 = R^3 = Br$
$Tp^{*,Br}$: $R^1 = R^3 = Me$; $R^2 = Br$
Tp^{Me3}: $R^1 = R^2 = R^3 = Me$
Tp^{Me2}: $R^1 = R^3 = Me$; $R^2 = H$
Tp^{Ph}: $R^1 = R^2 = H$; $R^3 = Ph$

oxidation of benzene into phenol using H_2O_2 as oxidant.[11] We herein report the results obtained in the course of our investigations on expanding the above catalytic system to alkanes. We have discovered that these hydrocarbons may undergo catalytic dehydrogenation and subsequent formation of alkenes. The transformation takes place under mild conditions, and the oxidant also operates as the sacrificial hydrogen acceptor, providing water as byproduct. With hexane as the alkane, the dehydrogenation seems to be preferred toward 1-hexene. Although conversions into alkenes at this stage of research are yet low, we believe that this is a proof of concept that copper-based catalysts, much cheaper than iridium, could be developed for this purpose.

RESULTS AND DISCUSSION

Oxidation of Cycloalkanes with Hydrogen Peroxide in the Presence of Tp^xCu Complexes. In our first set of experiments, we tested the catalytic capabilities of five copper complexes bearing different Tp^x ligands (Table 1). In all cases, we observed the formation of cyclohexanol as well as some cyclohexanone derived from overoxidation of the former

Table 1. Cyclohexane Oxidation Using Tp^xCu as Catalysts[a]

			dehydrog. products (%)		hydroxylated products (%)	
entry	catalyst	yield (%)	P1	P2	P3	P4
1	$Tp^{Br3}Cu$	22	4	3	45	48
2	$Tp^{*,Br}Cu$	11	4	4	27	65
3	$Tp^{*}Cu$	22	2	3	43	52
4	$Tp^{Me3}Cu$	21	1	3	43	53
5	$Tp^{Ph}Cu$	13	4	2	39	55
6	$Tp^{Br3}Cu^b$	24.5	3	2	38	57
7	$Tp^{Br3}Cu^c$	20	<1	2	56	41
8	$Tp^{Br3}Cu^d$	11	nd	2	54	44
9	$Tp^{Br3}Cu^e$	9	1	7	27	65

[a]Conditions: 0.01 mmol of catalyst, 3 mL MeCN, 1 mmol of cyclohexane, 10 mmol of H_2O_2, rxn time = 1 h, temp = 60 °C. See Scheme 4 for products numbering. Average of at least two runs. Conversions correspond to mmol of products/mmol of initial hydrocarbon. [b]rt, 7 h. [c]rt, 12 h. [d]rt, 24 h. [e]80 °C, 1 h.

(Scheme 4). Surprisingly we also observed the appearance of two minor products that have been identified as cyclohexene

Scheme 4. Products Observed in the Tp^xCu-Catalyzed Cyclohexane Oxidation Reaction

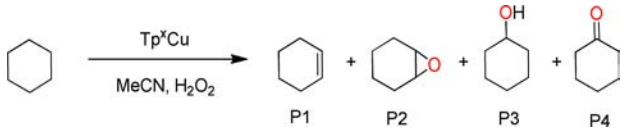

and cyclohexene oxide. Blank experiments revealed that cyclohexene was formed during the reaction of cyclohexane and hydrogen peroxide only in the presence of the copper catalysts (no cyclohexene was found upon reacting cyclohexane and H_2O_2 in the absence of Tp^xCu) and that cyclohexene epoxidized under the reaction conditions. It is also worth pointing out that no cyclohexene was detected as an impurity in the cyclohexane employed as substrate.

Table 1 shows the results obtained with the array of catalysts employed, after 1 h of stirring at 60 °C a 1:100:1000 mixture of $[Cu]:[C_6H_{12}]:[H_2O_2]$. All the complexes tested led to the formation of the four products shown in Scheme 4, but in a different ratio. The products derived from the dehydrogenation of cyclohexane, i.e., cyclohexene and cyclohexene oxide were minor (4–8% of the distribution of products). This behavior was not exclusive of cyclohexane, since the same protocol applied to cyclooctane led to the observance of cyclooctene, cyclooctene oxide and cyclooctenone (Scheme 5).

From the results in Table 1, entries 1–5, we chose $Tp^{Br3}Cu$ as the catalyst of choice, since it provided the best conversions as well as yields into the dehydrogenated products. A somewhat intriguing trend is observed when increasing the reaction time

Scheme 5. Oxidation of Cyclooctane with the $[Cu]/H_2O_2$ Catalytic System

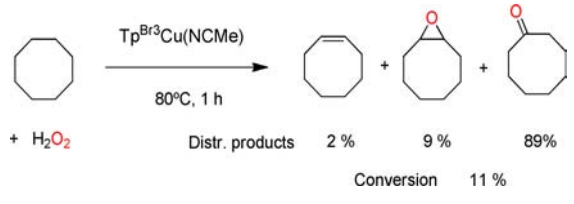

dx.doi.org/10.1021/ja310866k | J. Am. Chem. Soc. 2013, 135, 3887–3896

from 7 to 12 and 24 h: the yield values (intended as mmol of products/mmol of initial cyclohexane) decreased with time (Table 1, entries 6–8). In the same way, the reaction carried out at 80 °C resulted in a lower yield than that observed at 60 °C (entries 1 vs 9). We have learnt that this is due to cyclohexane loss by diffusion into the vapor phase (see Supporting Information)

The reaction of cycloalkanes with hydrogen peroxide in the presence of transition metal complexes has been previously described by several groups,[12] although in no case dehydrogenation was reported. It has been proposed that those transformations seem to occur under Fenton-like pathways, i.e., with the intermediacy of free hydroxyl radicals. Later on this manuscript, we will provide mechanistic studies demonstrating that this statement does not apply in our case, with metal-oxo species being responsible of the observed transformations.

Oxidation of *n*-Hexane. At this stage we wondered if a linear alkane such as n-hexane could undergo this transformation.[13] Initially, and on the basis of the reactions with cycloalkanes, we could expect the products derived from (i) C–H hydroxylation, (ii) oxidation of the alcohol to give aldehyde or ketone, (iii) dehydrogenation, and (iv) oxidation of the olefin to the oxide. Scheme 6 shows the 12 possible products,

Scheme 6. Oxidation of *n*-Hexane with the [Cu]/H_2O_2 Catalytic System Showing All Possible Products[a]

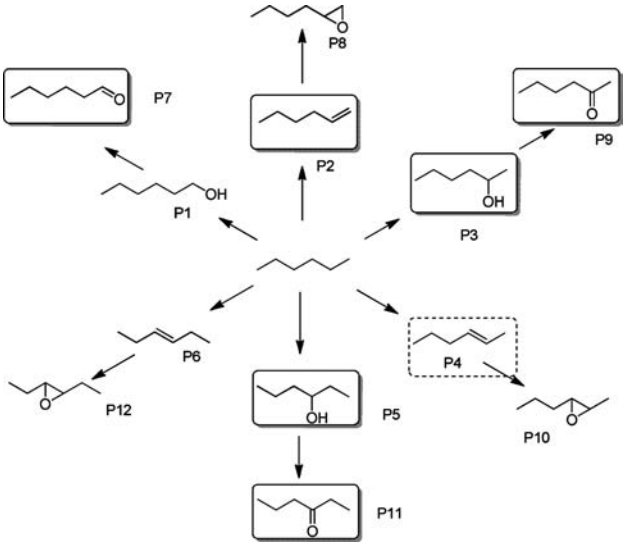

[a]Detected products are framed. See Table 2 for distribution of products.

from which we have identified seven in variable amounts (Table 2), by comparison with commercial samples using GC/GCMS techniques. Hydroxylation products and their overoxidation derivatives were the main outcome of the reaction, particularly that yield by the functionalization of the internal C2–H and C3–H bonds. Primary sites were also oxidized, and 1-hexanal was detected as the result of the oxidation of 1-hexanol. Regarding the dehydrogenation reaction, 1-hexene was formed as the sole olefin in most experiments. Only in a single case, 2-hexene was detected at very low concentration (Table 2, entry 4). No epoxides were detected in the reaction mixture. Therefore, this catalytic system induces the dehydrogenation of not only cycloalkanes, but also of less reactive alkanes such as

Table 2. Oxidation of *n*-Hexane with H_2O_2 and $Tp^{Br3}Cu(MeCN)$ as the Catalyst[a]

entry	mmol H_2O_2	yield (%)	P2	P3	P4	P5	P7	P9	P11
1	5	6.5	5	–	–	–	12	42	41
2	10	7	10	–	–	–	8	36	45
3[b]	10	8.5	9	9	–	8	7	34	33
4[c]	10	6.5	>9	–	<2	1	9	38	41
5[d]	10	5	5	–	–	3	5	41	46

[a]See Scheme 6 for numbering. 0.01 mmol of catalyst, 3 mL of MeCN, 1 mmol of hexane, rxn time = 1 h, temp = 60 °C. Average of at least two runs. Yield values correspond to mmol of products/initial mmol of hydrocarbon. [b]Rxn time = 3.5 h, at rt. [c]Rxn time = 5 h, at rt. [d]Rxn time = 12 h, at rt.

n-hexane. As mentioned in the Introduction, this dehydrogenation process in which an oxidant is employed has only been reported with manganese in a catalytic manner,[5,6] and using substrates in which the dehydrogenation of activated (benzylic) C–H bonds also induces the aromatization of the resulting product. In our case, loss of hydrogen takes place in nonactivated C–H bonds, where there is not such a driving force similar to aromatization. The use of copper as the metal center and hydrogen peroxide as the oxidant are also novel for this transformation.

Oxidation of Dihydroaromatic Substrates. For the sake of completeness, we have evaluated our catalytic system with the substrates previously described by Crabtree[5] and Yin[6] with manganese-based catalysts (as shown in Scheme 2). In our case, both dihydrophenanthrene and dihydroanthracene were dehydrogenated to give phenanthrene and anthracene (Scheme 7), respectively, along with oxidation products. Conversions of

Scheme 7. Distribution of Products of 9,10-Dihydrophenanthrene (Top) and Dihydroanthracene (Bottom) Oxidation Reactions

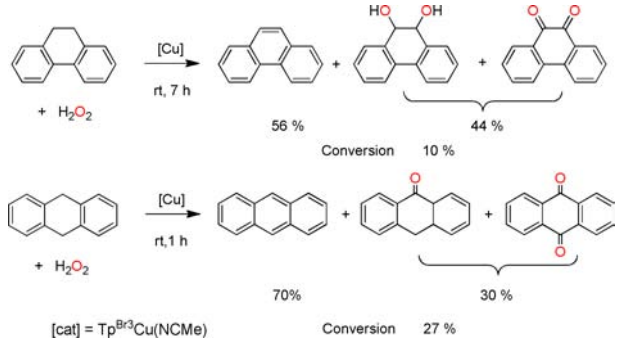

10 and 27% (based on initial hydrocarbon) were obtained using hydrogen peroxide with this copper-based catalyst, at variance with PhIO or $KHSO_5$ that were employed in those studies.

Mechanistic Studies. *Evidencing the Lack of Fenton-Like Pathways.* A well-known feature of many transition metals is the capability to promote the decomposition of hydrogen peroxide and the generation of hydroxyl radicals ($HO^{\bullet}$) that further induces oxidation reactions.[14] This is the base of the so-called Fenton chemistry,[15] that is mainly characterized by the lack of selectivity. Since several copper compounds or salts have been reported to generate such radical promoting alkane oxidations,[12,16] we have first performed a series of experiments to elucidate whether or not our transformation occurs in a

dx.doi.org/10.1021/ja310866k | J. Am. Chem. Soc. 2013, 135, 3887–3896

similar manner. However, we must emphasize at this point that *no alkene formation has ever been described in those copper-based systems.*

The previous copper-based catalytic systems for cycloalkane hydroxylation are dominated by the proposal of the participation of hydroxyl radicals (Scheme 8) that induce

Scheme 8. Previously Proposed Free-Radical Copper Induced Oxidation of Cyclohexane

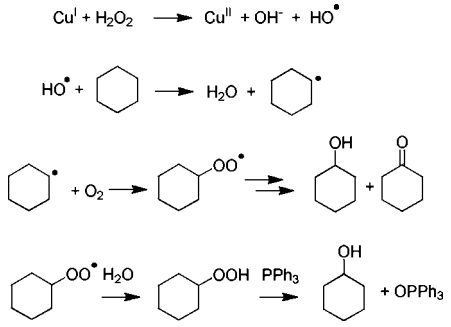

hydrogen abstraction from the cycloalkane.[12,16] The cyclohexyl radical is further trapped by molecular oxygen to give the alkylperoxide radical, from which cyclohexanol and cyclohexanone are formed after several steps. Under the conditions employed, cyclohexylperoxide is also formed. The latter can be easily converted into cyclohexanol in a selective manner upon addition of PPh_3 (Scheme 8), in what is considered[12a] a probe to demonstrate the involvement of a peroxidative process triggered by hydroxyl radicals. A second probe is the use of an inert atmosphere,[16a] which should decrease the yield into oxidation products since molecular oxygen is required for cycloalkylperoxide formation.

In our system, we have collected some experimental data related to the above. First of all, we have not observed any variation of the reaction outcome upon varying the atmosphere from air to nitrogen. Also, following the established protocols,[12a,16] we have carried out experiments in which twin reactions were run, and PPh_3 was added at the end to one of each couple. As shown in Table 3, the catalytic results did

Table 3. Effect of the Addition of PPh_3 in the Reaction of Cyclohexane and H_2O_2 Using $Tp^{Br3}Cu(NCMe)$ as the Catalyst[a]

			dehydrog. products (%)		hydrox. products (%)	
entry	catalyst	yield (%)	P1	P2	P3	P4
1	$Tp^{Br3}Cu$	22%	3.5	3	45	48.5
2[b]	$Tp^{Br3}Cu$	21%	3	2	50	45

[a]Conditions: 0.01 mmol of catalyst, 3 mL of MeCN, 1 mmol of cyclohexane, 10 mmol H_2O_2, rxn time = 1 h, temp = 60 °C, see Scheme 4 for products numbering. Conversion values correspond to mmol of products/initial mmol of hydrocarbon. [b]Values determined by GC after addition of 0.5 mmol of PPh_3.

not vary when comparing the results in the presence or absence of PPh_3. From here we could conclude that no cycloalkylperoxides derived from the action of HO• radicals are formed in our system. However, it could happen that our copper catalyst would also induce the catalytic decomposition of the cycloalkylhydroperoxide in an efficient manner in such a way that the experiment with PPh_3 would not be informative. Although this behavior has not been reported with copper, Lyons et al described this effect with iron-based catalysts.[17]

In our search for additional evidence that could provide information about the nature of the mechanism governing this transformation, we have taken advantage of the already described catalytic capabilities of these Tp^xCu complexes to oxidize aromatic C−H bonds.[11] In our previous report on this reaction, we observed that the reaction with benzene led to the *exclusive* formation of phenol and benzoquinone. It has been established that the oxidation of phenol with the intermediacy of the hydroxyl radical also produces biphenyl derivatives as the result of the coupling of the phenyl radical, but we have not detected this product in our system. To reinforce this data, we have now studied the reaction of toluene and H_2O_2 with $Tp^{*,Br}Cu(NCMe)$ as the catalyst. GC and GCMS studies have revealed the formation of a mixture of compounds identified as benzaldehyde, *ortho*- and *para*-cresols and 2-methyl-1,4-benzoquinone (Scheme 9). The oxidation of toluene by the

Scheme 9. Oxidation of Toluene with Hydrogen Peroxide Using $Tp^{*,Br}Cu(NCMe)$ as the Catalyst

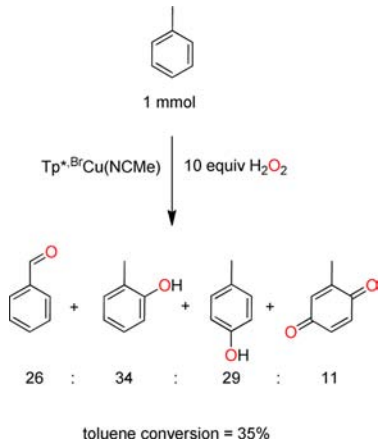

hydroxyl radical is known to produce biaryl derivatives,[15] which we have not detected in the reaction mixtures. In contrast, the distribution of products obtained with our copper catalyst (Scheme 9) was similar to that found by Sawyer and co-workers,[18] where they proposed that some iron-based catalysts for these transformations did not operate throughout the HO• route. Other groups have already found evidence against the involvement of hydroxyl radicals in this catalytic process.[19] Particularly, studies by Marusawa, Tezuka and co-workers demonstrated[19b] that the distribution of cresols derived from photolytically generated HO• radicals and toluene was 71:9:20 for *o*:*m*:*p*-cresols, a set of values quite distinct from those in Scheme 9 (ca. 61:0:39, counting the quinone as derived from the *ortho* derivative).

Overall, data collected and presented above seem to disfavor the proposal of the involvement of free HO• radicals in this process.

Evidencing the Intermediacy of Copper-Oxo Species. The use of oxone, which contains $KHSO_5$ as the oxidant, has also provided valuable information since it does not produce hydroxyl radicals.[20] The reaction of cyclohexane and oxone in the presence of catalytic amounts of these copper complexes originates a mixture of cyclohexanol and cyclohexanone, as well as cyclohexene as the minor product, with yields similar to those observed with hydrogen peroxide as the oxidant (Scheme

dx.doi.org/10.1021/ja310866k | J. Am. Chem. Soc. 2013, 135, 3887−3896

10). These results suggest that both hydrogen peroxide and oxone involve a similar reaction mechanism in the copper-catalyzed oxidation of cyclohexane.

Scheme 10. Oxidation of Cyclohexane with Oxone in the Presence of the Copper Catalyst

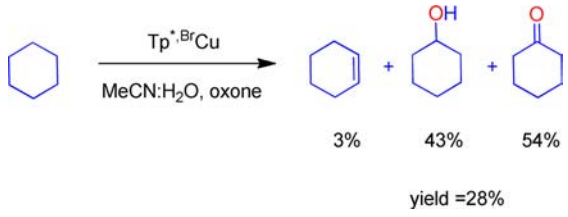

Additional as well as crucial information has been found when radical inhibitors when employed. The use of commonly employed radical inhibitors such as 2,6-ditertbutyl-4-methyl-phenol (BHT) or TEMPO was precluded since under the reaction conditions (copper source and hydrogen peroxide) they were also oxidized, due to the presence of either aromatic or aliphatic C−H bonds. Thus, we moved toward radical traps not having C−H bonds such as CCl_4 or $CBrCl_3$. When the reaction was carried out in the presence of added CCl_4, some cyclohexyl chloride was detected at the end of the reaction (Scheme 11). This is in good agreement with the generation of

Scheme 11. The Effect of Added CCl_4 or $CBrCl_3$ to the $Tp^{Br3}Cu$-Catalyzed Reaction of Cyclohexane and H_2O_2

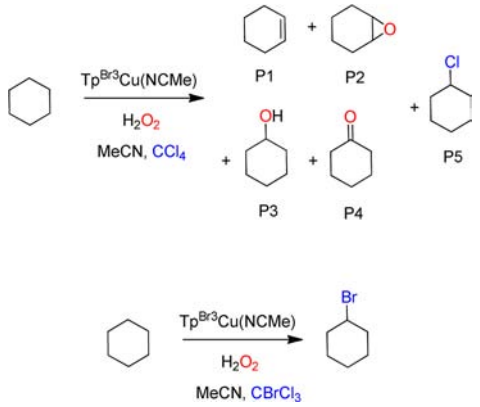

the $C_6H_{11}^{\bullet}$ radical, as demonstrated by Mansuy and co-workers in the related nitrene transfer reaction.[21] Moreover, when the chlorinated additive was changed to $CBrCl_3$, then the main product was bromocyclohexane, the oxidation/dehydrogenation products being detected in very minor amounts (<1% overall). A recent work by Shaik, Nam and co-workers[8] with a Fe(IV)═O complex has shown that the alkyl radical formed upon H-abstraction from the alkane is similarly trapped with $CBrCl_3$. Therefore, our data seem to support the involvement of a copper-oxo species that abstracts a hydrogen from cyclohexane yielding cyclohexyl radicals that are trapped by halogenated reagents. The validity of this proposal has been checked by the theoretical studies presented in the following section.

Mechanistic Studies: DFT Calculations. The aforementioned previous work by Crabtree, Eisenstein and co-workers[5b] has established the existence of two competing pathways (Scheme 12) involving the formation of a carbon-radical

Scheme 12. Previously Proposed Pathways for the C−H Bond Hydroxylation/Desaturation Reactions

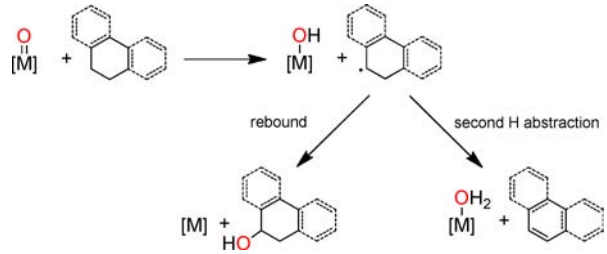

species, which yields hydroxylation/desaturation product mixtures. In the hydroxylation pathway, the OH group couples with that radical, following the rebound mechanism, whereas in the desaturation pathway, the vicinal C−H bond undergoes a second H abstraction. Both pathways are initiated by a common metal-oxo intermediate. Late transition metal oxo complexes are extremely reactive and thus difficult to isolate and characterize. Nonetheless, these complexes have been proposed as active species in several catalytic systems[22] and characterized for a few metal−ligand combinations able to provide enough stability to the system.[23]

To collect some additional information about the mechanism that governs this transformation, the reaction mechanism was explored by means of DFT calculations on the oxidation of cyclohexane by the $Tp^{Br3}Cu$ catalyst (see Computational Details). The full real structures of the substrate and the catalyst were considered without any simplifications. Free energies in solution, G_{sol}, were computed by including both the solvent effects of acetonitrile (at the CPCM level with a triple-ζ basis set) and the thermochemistry corrections (zero-point, thermal and entropy energies).

Scheme 13 shows the three possible species that can be formed upon oxidation of the catalyst precursor with hydrogen

Scheme 13. Possible Copper Active Species Considered in This Study

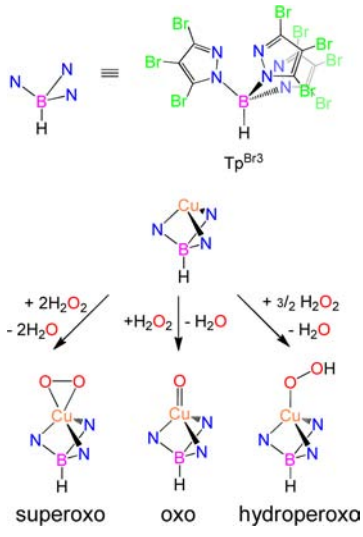

peroxide: the copper oxo, superoxo and hydroperoxo species.[24] We have investigated them as potential active species, calculating the stability and reactivity with cyclohexane.

We have started optimizing the singlet and triplet states of the oxo species, **S** and **T**, respectively. The ground state is the

dx.doi.org/10.1021/ja310866k | J. Am. Chem. Soc. 2013, 135, 3887−3896

triplet, which lies 33.2 kcal mol^{-1} below the singlet. The coordination geometry of the ground state is tetrahedral, with the trispyrazolylborate ligand bound to copper in a κ^3 fashion. The formation of the oxo species from the catalyst and hydrogen peroxide (Scheme 13) is exergonic, ΔG = −3.6 kcal mol^{-1}. Cyclohexane interacts with **T** yielding intermediate **T-1**, in which a C−H bond of the substrate is weakly H-bonded to the oxygen ligand, d(H···O) = 2.56 Å. This species, which is similar to the prereaction complex characterized by Costas et al. for C−H oxidation by Mn(IV)=O species,[25] lies 7.0 kcal mol^{-1} below reactants (Figure 1). The local spin densities on

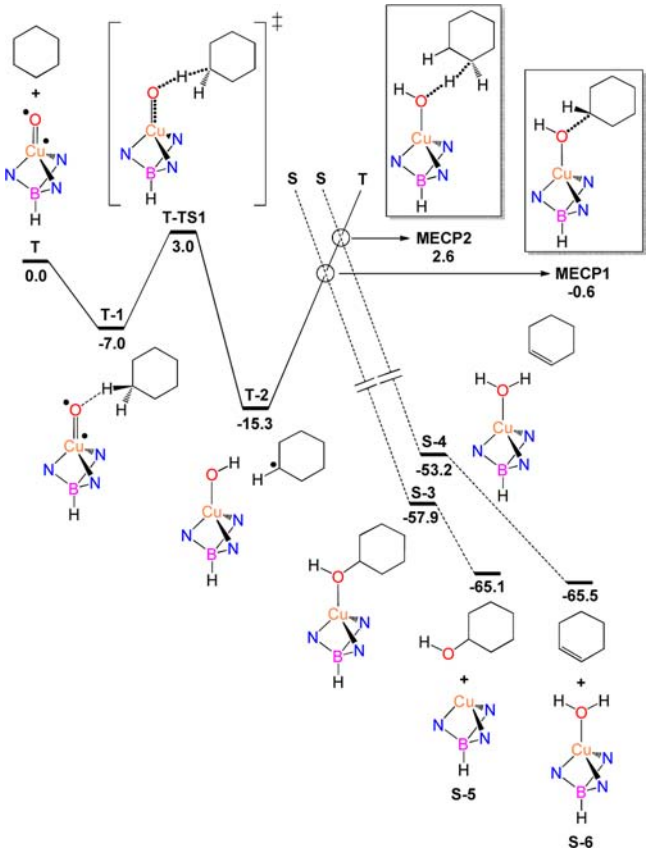

Figure 1. Gibbs energy (G_{sol}) profile in acetonitrile (kcal mol^{-1}), for the hydroxylation and dehydrogenation of cyclohexane in the triplet (solid line) and singlet (dashed line) states for the copper-oxo species.

copper and oxygen, ρ(Cu) = 0.80 and ρ(O) = 1.11 (Table 4 and Figure 2), are more consistent with a radical Cu^{II}−O$^{\bullet}$ configuration, referred to as oxyl,[26] than with a closed-shell Cu^{III}=O oxo.

The oxyl character of **T-1** may promote radical H abstraction reactions.[27] The transition state of this reaction, **T-TS1**, was located at a relative energy of 3.0 kcal mol^{-1} (Figure 1). In **T-TS1**, the H-bound C−H of **T-1** breaks, d(C···H) = 1.25 Å, and transfers the H atom to the oxyl ligand, d(H···O) = 1.25 Å (Figure 3). The oxyl spin density is reduced to ρ(O) = 0.68, due to its polarization toward the activated C−H bond, which gains radical character on its C atom, ρ(C) = 0.47 (Table 4 and Figure 2). This is consistent with the pairing of two electrons to form the new O−H bond, one coming from the oxyl and the other from the homolytic cleavage of the C−H bond. The relaxation of **T-TS1** toward products converged into intermediate **T-2**, which is a copper-hydroxo complex weakly

Table 4. Local Spin Densities (ρ)[a] and Charges (q) of the Stationary Points Involved in the H Abstraction Step

	T-1	T-TS1	T-2
ρ(Cu)	0.80	0.81	0.84
ρ(O)	1.11	0.68	0.10
ρ(C)[b]	0.00	0.47	0.96
ρ(H)[b]	0.00	−0.06	−0.01
ρ(C_6H_{11})	0.00	0.48	0.97
ρ(Tp^{Br3})	0.09	0.09	0.10
q(Cu)	1.13	1.17	1.18
q(O)	−0.65	−0.94	−1.14
q(C)[b]	−0.38	−0.23	−0.09
q(H)[b]	0.21	0.29	0.47
q(C_6H_{11})	−0.21	−0.01	0.00
q(Tp^{Br3})	−0.48	−0.51	−0.51

[a]Positive and negative spin densities are alpha and beta, respectively. [b]C and H belong to the activated C−H bond of cyclohexane.

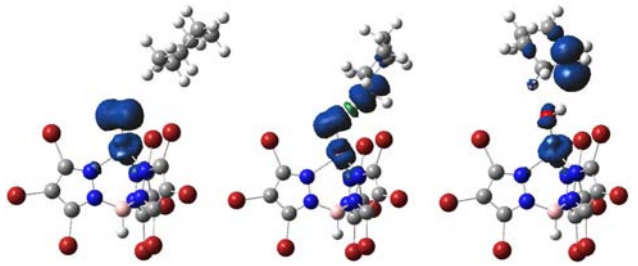

Figure 2. Spin densities of **T-1** (left), **T-TS1** (middle) and **T-2** (right). Spin density colors: blue (alpha), green (beta). Atom colors: orange (Cu), red (O), white (H), gray (C), blue (N), maroon (Br), purple (B).

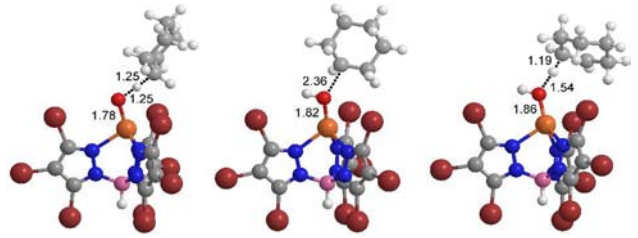

Figure 3. Optimized geometries of **T-TS1** (left), **MECP1** (middle), and **MECP2** (right). Atom colors: orange (Cu), red (O), white (H), gray (C), blue (N), maroon (Br), purple (B).

associated with the C_6H_{11} organic fragment. This fragment corresponds to the neutral cyclohexyl radical, $C_6H_{11}^{\bullet}$, as shown by its local charge, q(C_6H_{11}) = 0.00, and spin density, ρ(C_6H_{11}) = 0.97, which is concentrated upon the C involved in the C−H cleavage, ρ(C) = 0.96. The generation of this radical is consistent with the formation of $C_6H_{11}Cl$ in the presence of CCl_4 or of $C_6H_{11}Br$ in the presence of $CBrCl_3$ (Scheme 11) and the preferential oxidation of the secondary carbons of *n*-hexane (Scheme 6), which stabilize the radical more than the primary. The metal center and the Tp^{Br3} ligand seem to play a somewhat spectator role, since their local charges and spin densities are almost constant throughout the reaction. Starting from **T-1**, the H abstraction step is exergonic by 8.3 kcal mol^{-1} and involves a low energy barrier of 10.0 kcal mol^{-1}. The triplet state of the oxo species thus initiates the oxidation of cyclohexane by a radical H abstraction.

dx.doi.org/10.1021/ja310866k | J. Am. Chem. Soc. 2013, 135, 3887−3896

The reactivity of the Cu^{II} superoxo and hydroperoxo complexes (Scheme 13), which may also act as active species,[24] was investigated for this H abstraction process. The formation of these species from the catalyst and hydrogen peroxide is more exergonic than that of the oxo, with $\Delta G = -56.5$ kcal mol^{-1} (superoxo) and $\Delta G = -27.3$ kcal mol^{-1} (hydroperoxo). Similar to the oxo species, the superoxo abstracts one hydrogen from cyclohexane, yielding the cyclohexyl radical (see Figures S11 and S12 in the Supporting Information). However, the barrier associated with this reaction, $\Delta G^{\ddagger} = 32.4$ kcal mol^{-1}, is higher than that given by the oxo, $\Delta G^{\ddagger} = 10.0$ kcal mol^{-1}. The hydroperoxo complex also involves a higher energy barrier, $\Delta G^{\ddagger} = 27.3$ kcal mol^{-1}, and, in contrast with the oxo and the superoxo, promotes the reaction through a concerted mechanism, inconsistent with the formation of cyclohexyl radicals shown by the experiments (Scheme 11).

These results suggested that the superoxo and hydroperoxo complexes are more stable but less reactive than the oxo, as previously reported for similar systems.[24a,b] In addition, our experiments suggest that the reaction follows the same mechanism when either oxygen is excluded or hydrogen peroxide is replaced by oxone (vide supra). Under these conditions, the formation of peroxidic complexes is unlikely. These complexes were thus excluded as active species and the theoretical investigations focused on the oxidation of the cyclohexyl radical to cyclohexanol from intermediate **T-2** on the oxo pathway (Figure 1). In the classical rebound mechanism, the organic radical abstracts the OH ligand of the hydroxo intermediate.[28] All attempts to optimize the transition state of this reaction in the triplet state led to high-energy nonconverged geometries. This is due to the need of switching the spin state[29] from the triplet of **T-2**, which can be formulated as $[Tp^{Br3}Cu^{\bullet}(OH)]C_6H_{11}^{\bullet}$ (Figure 1), to the singlet of **S-3**, $[Tp^{Br3}Cu(C_6H_{11}OH)]$, which is a closed-shell Cu^{I} d^{10} species. We located the minimum energy crossing point (MECP) associated with this spin crossover, **MECP1** (Figure 3), which has a geometry very similar to that of the classical OH rebound transition state.[30] In **MECP1**, the formation of the C−O bond, d(C···O) = 2.36 Å (3.46 Å in **T-2**), is accompanied by the elongation of the Cu−O bond, d(Cu···O) = 1.82 Å (1.78 Å in **T-2**). The relaxation of **MECP1** in the triplet and singlet states yielded the expected **T-2** and **S-3** intermediates, respectively. In **S-3**, the cyclohexanol product is formed and coordinated to the metal center, d(C−O) = 1.43 Å and d(Cu···O) = 2.06 Å.

The spin density surface of **T-2** revealed the presence of some radical oxyl character in the OH ligand (Figure 2). The value of ρ(O) is rather small, 0.10 (Table 4), but this has been proven to be enough to promote dehydrogenation by double H abstraction.[5] In addition, Solomon and co-workers have recently shown the active role of copper-hydroxo species in C−H oxidation.[31] This prompted the location of an alternative MECP for the formation of cyclohexene, **MECP2** (Figure 3). The geometrical parameters of this MECP are consistent with the cleavage of the C−H bond, d(C···H) = 1.19 Å (1.09 Å in **T-2**), accompanied by the transfer of H to O, d(H···O) = 1.54 Å (2.65 Å in **T-2**). The Cu−O bond elongates to 1.86 Å (1.78 Å in **T-2**) and the C−C bond shortens to 1.43 Å (1.49 Å in **T-2**). The full optimization of **MECP2** in the triplet and singlet states yielded intermediates **T-2** and **S-4**, respectively, with the latter containing the cyclohexene product, d(C=C) = 1.33 Å. The spin stability reversal around **MECP1** and **MECP2** was confirmed by single point calculations. Intermediate **T-2** is 60.3 kcal mol^{-1} less stable in the singlet state, whereas **S-3** and **S-4** are 88.2 kcal mol^{-1} and 83.7 kcal mol^{-1}, respectively, less stable in the triplet state.

The release of cyclohexanol, $\Delta G = -7.2$ kcal mol^{-1} from **S-3**, and cyclohexene, $\Delta G = -12.3$ kcal mol^{-1} from **S-4**, is exergonic. The overall hydroxylation and dehydrogenation reactions are much more exergonic, $\Delta G = -65.1$ kcal mol^{-1} and $\Delta G = -65.5$ kcal mol^{-1}, respectively. The energy landscape depicted in Figure 1 suggests that the reaction becomes irreversible after spin crossover, which is thus determining the final outcome of the reaction. Given the rather small energy difference between **MECP1** and **MECP2**, 3.2 kcal mol^{-1}, a mixture of cyclohexanol and cyclohexene is expected, with the former being the major product. Further refinement with the dispersion-corrected DFT functionals MPWB1K and M06-2X gave energy differences of 1.0 and 1.3 kcal mol^{-1}, respectively. These values are in good agreement with the hydroxylation:desaturation ratio observed in the experiments, 93:7 at 60 °C (entry 1 in Table 1), which would correspond to an energy difference of 1.7 kcal mol^{-1}, thus suggesting that dispersion may play a role in the selectivity of these reactions. A recent work by Shaik and co-workers[32] has shown that ancillary ligand flexibility influences the hydroxylation/dehydrogenation ratio. In our case, the trispyrazolylborate ligand is quite rigid along the pathway and seems to exert no influence in the reaction outcome.

The low energy profiles found for the oxidation of cyclohexane (Figure 1) support the participation of the oxo complex (Scheme 13) as active species. For the sake of completeness, we also investigated the formation of this complex for the $Tp^{*,Br}$ ligand (Figure S13). After the initial coordination of hydrogen peroxide to the metal center, spin crossover from the singlet to the triplet state causes the cleavage of the O−O bond, leading to the formation of a bis-hydroxo intermediate, similar to the water oxidation catalyst recently reported by Mayer and Goldberg.[33] This species undergoes intramolecular proton transfer followed by water decoordination, yielding the oxo complex. At 22.9 kcal mol^{-1} above reactants, the MECP for spin crossover is the highest energy point along this reaction pathway, which, overall, is exergonic by 10.1 kcal mol^{-1}. These energies suggest that the formation of the postulated oxo active species is feasible under the mild conditions used in our experiments (vide supra).

Mechanistic Proposal. On the basis of the experimental and theoretical data, we have built the mechanistic proposal shown in Scheme 14. The $Tp^{x}Cu$ core reacts with hydrogen peroxide to give a copper-oxo intermediate with strong oxyl character. Interaction with cyclohexane induces a hydrogen abstraction process yielding the cyclohexyl radical and $Tp^{x}Cu$−OH. From here, two competitive pathways may occur. Through the hydroxylation pathway (Scheme 14b), the cyclohexyl radical collapses with $Tp^{x}Cu$−OH leading to cyclohexanol formation, whereas through the dehydrogenation pathway (Scheme 14a), a second hydrogen abstraction from the α C−H of the cyclohexyl radical leads to cyclohexene formation. In the latter case, the oxidant itself acts as hydrogen acceptor, with the net reaction providing two molecules of water from one molecule of H_2O_2 and cyclohexane. These pathways involve spin crossover through MECPs of similar energy, which leads to product mixtures. The lowest-energy MECP yields cyclohexanol as major reaction product. None of these pathways involve the formation of free hydroxyl radicals.

dx.doi.org/10.1021/ja310866k | J. Am. Chem. Soc. 2013, 135, 3887−3896

Scheme 14. Mechanistic Proposal for the Copper-Catalyzed Oxidation of Cyclohexane Showing the Two Competitive Pathways

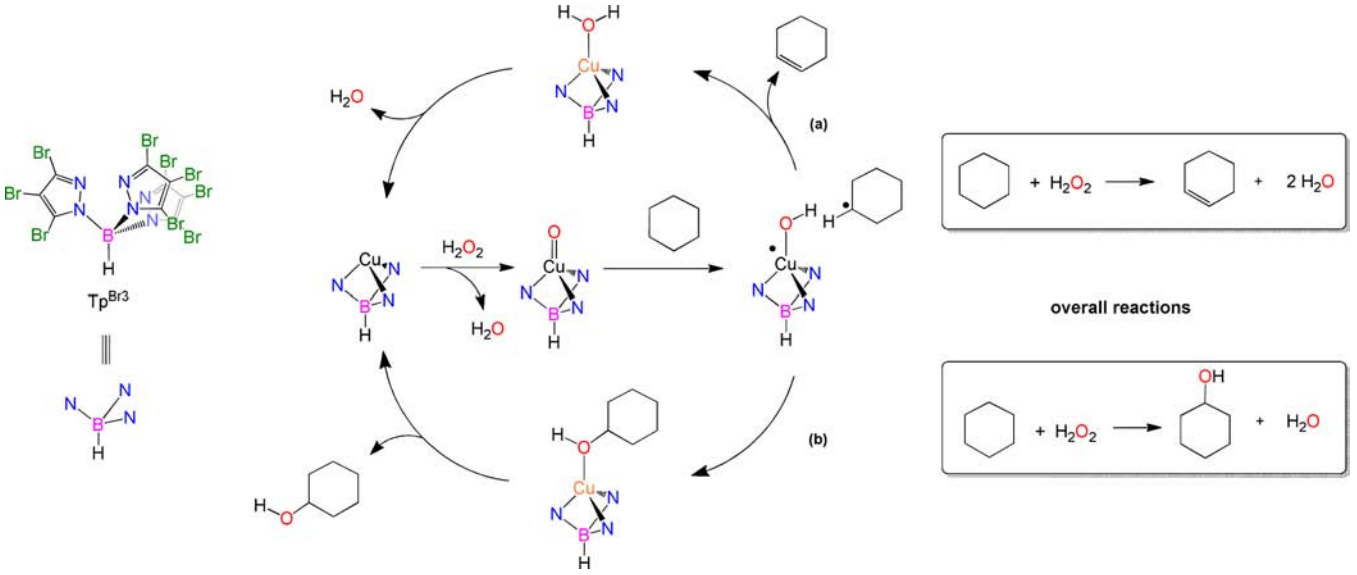

CONCLUSIONS

In summary, we have discovered that the complexes [Tp^{x}Cu(NCMe)] catalyze the oxidation of nonactivated alkane C−H bonds providing alcohols and/or ketones as the major products but inducing the unprecedented dehydrogenation of these substrates with copper under mild reaction conditions. With *n*-hexane as the substrate, 1-hexene has been formed upon such dehydrogenation process, with other olefins being undetected in most cases. The use of the above hydrocarbons as substrates, of copper as catalyst, and of hydrogen peroxide as oxidant is novel in this kind of transformation. Experimental data as well as DFT calculations suggest a competitive mechanism in which the hydroxylation and dehydrogenation pathways are initiated from a common oxo intermediate. Work aimed at designing new catalysts for selective dehydrogenation is currently underway in our laboratories.

EXPERIMENTAL SECTION

General. All catalytic experiments were carried out under air. The chemicals were purchased from Aldrich and were used without previous purification. The Tp^x ligands[10] and the complexes [Tp^{x}Cu(NCMe)][34] were prepared according to the literature procedures. NMR data were recorded in a Varian Mercury 400 spectrometer. GC and GCMS data were collected with a Varian GC-3900 with a FID detector or a Varian Saturn 2100, respectively.

General Catalytic Oxidation Procedure. The reactions were performed in a 25 mL round bottomed flask equipped with a reflux condenser and a magnetic stirrer bar. In a typical experiment (for other conditions, see the footnotes of Tables 1 and 2), 0.01 mmol of catalyst was dissolved in 3 mL of acetonitrile and 1 mmol (108 μL) of cyclohexane and 10 mmol (1 mL) of an aqueous commercial solution of hydrogen peroxide (30% v/v) were added in one portion. The mixture was stirred for 1 h at 60 °C. After cooling at room temperature, additional dichloromethane (2 × 2.5 mL) was added to extract the organic products. Cycloheptanone was added as internal standard and the mixture was directly analyzed by GC and GCMS to determine the mass balance, the conversion and relative ratio of products by comparison with commercial samples (see Supporting Information).

Catalytic Procedure Using PPh_3 as Additive. The reactions were performed in a 25 mL round bottomed flask equipped with a reflux condenser and a magnetic stirrer bar. In a typical procedure, 0.01 mmol of catalyst was dissolved in 3 mL of acetonitrile and 1 mmol (108 μL) of cyclohexane and 10 mmol (1 mL) of an aqueous commercial solution of hydrogen peroxide (30% v/v) were added in one portion. The mixture was stirred for 1 h at 60 °C. After cooling at room temperature, PPh_3 was added (0.5 mmol), and the reaction mixture was stirred 20 min. Additional dichloromethane (2 × 2.5 mL) was then added to extract the organic products. The reaction was then investigated by GC as described above.

Catalytic Oxidation of Cyclohexane in the Presence of CCl_4 or $CBrCl_3$. The reaction was performed in a 25 mL round bottomed flask equipped with a reflux condenser and a magnetic stirrer bar. In a typical procedure, 0.01 mmol of catalyst was dissolved in 2.5 mL of acetonitrile and 0.5 mL of CCl_4 and 1 mmol (108 μL) of cyclohexane and 10 mmol (1 mL) of an aqueous commercial solution of hydrogen peroxide (30% v/v) were added in one portion. The mixture was stirred for 1 h at 60 °C. After cooling at room temperature, additional dichloromethane (2.5 mL) was added to extract the organic products. Analysis of the final reaction mixture was done by GC with the above protocol. The reaction with $CBrCl_3$ was performed in a similar manner using 3 mL of acetonitrile and 1 mmol of $CBrCl_3$ (ca. 0.1 mL). See Supporting Information for GC traces.

Catalytic Procedure of Toluene Oxidation. The reactions were performed in a 25 mL round bottomed flask equipped with a reflux condenser and a magnetic stirrer bar. In a typical experiment, 0.01 mmol of catalyst was dissolved in 1 mL of acetonitrile and 1 mmol (106 μL) of toluene and 10 mmol (1 mL) of an aqueous commercial solution of hydrogen peroxide (30% v/v) were added in one portion. The mixture was stirred for 8 h at 75 °C. Additional dichloromethane (2 × 2.5 mL) was then added to extract the organic products. Styrene was added as internal standard and a sample of the mixture was directly analyzed by GC/GCMS as above.

Catalytic Procedure Using Oxone as Oxidant. The reactions were performed in an ampule. In a typical experiment, 0.02 mmol of catalyst was dissolved in 5 mL of acetonitrile and 30 mmol (3.24 mL) of cyclohexane. A solution of 0.5 mmol of oxone in 5 mL of water was added in one portion. The mixture was stirred for 72 h at 60 °C. Additional dichloromethane (2 × 2.5 mL) was then added to extract the organic products. Cycloheptanone was added as internal standard and a sample of the mixture was directly analyzed by GC/GCMS.

Computational Details. The calculations were carried out with Gaussian09[35] at the DFT(BHLYP)[36] level. Two distinct basis sets, BS-I and BS-II, were used. With BS-I, H, B, C, N and O were described with the all-electron double-ζ 6-31G** basis set,[37] whereas Br and Cu were described with the Stuttgart−Dresden basis set including scalar relativistic ECP.[38] With BS-II, H, B, C, N and O were described with the triple-ζ 6-311+G** basis set.[39] All stationary points were fully

dx.doi.org/10.1021/ja310866k | J. Am. Chem. Soc. 2013, 135, 3887−3896

optimized in gas phase with BS-I without any geometry or symmetry constraints. Harmonic frequencies were computed analytically with BS-I in order to classify the stationary points as either minima (reactants, intermediates and products) or saddle points (transition states). These calculations were also used to determine the difference between the Gibbs and potential energies, $(G - E)$, which includes the zero-point, thermal and entropy corrections. Hindered rotor calculations showed that the error associated with the lowest frequencies is smaller than 0.1 kcal mol^{-1}. The nature of the transition states was further confirmed by means of IRC calculations[40] with BS-I. The effect of the solvent, acetonitrile (ε = 35.688), was estimated by computing the CPCM energy,[41] E_{CPCM}, in single-point calculations with BS-II. All energies given in the text are Gibbs energies in solution, G_{sol}, which were calculated by adding the thermodynamic corrections to the CPCM energies (eq 2).[42]

$$G_{sol} = E_{CPCM} + (G - E) \quad (2)$$

The use of the hybrid BHLYP functional is based on previous studies by Sodupe and Rodríguez-Santiago.[43] In these studies, a series of copper-aqua complexes were studied with several DFT functionals, with BHLYP giving the most accurate results when compared to reference CCSD(T) calculations.[44] Two other functionals, the MPWB1K[45] and M06-2X[46] were also used to refine the critical energy difference between **MECP1** and **MECP2**. These functionals, which have an amount of HF exchange (44% in MPWB1K and 54% in M06-2X) similar to that of BHLYP (50%), were designed for an accurate description of dispersion forces.

The minimum energy crossing points (MECPs) were located with the program developed by J. N. Harvey.[29a] The nature of the MECPs was confirmed by their full optimization in each of the two spin states involved in the crossing. The thermodynamic and solvent corrections associated with the MECPs were evaluated by averaging the values found for each spin state. The local charges and spin densities were obtained from NPA calculations.[47]

■ ASSOCIATED CONTENT

Supporting Information

Detailed experimental catalytic and mechanistic procedures, including GC traces; computational data including Cartesian coordinates and energies of all stationary points reported in the text as well as further details on the reactivity of the superoxo and hydroperoxo species and the formation of the oxo active species; complete ref 35. This material is available free of charge via the Internet at http://pubs.acs.org.

■ AUTHOR INFORMATION

Corresponding Author

perez@dqcm.uhu.es; agusti@klingon.uab.es; mmdiaz@dqcm.uhu.es; david.balcells@kjemi.uio.no

Notes

The authors declare no competing financial interest.

■ ACKNOWLEDGMENTS

Dedicated to Prof. Gregorio Asensio on occasion of his 65th birthday. We thank MINECO (Proyectos CTQ2011-28942-CO2-01, CTQ2011-23336, Consolider Ingenio 2010, CSD2006-00003 and CSD2007-00006) and Fondos Feder for funding. D.B. and L.V. also thank MINECO for a Juan de la Cierva contract and a predoctoral fellowship, respectively. Junta de Andalucía (P10-FQM-06292) is also acknowledged for funding. D.B. thanks the Norwegian Research Council for financial support through the CoE Centre for Theoretical and Computational Chemistry (CTCC) Grant No. 179568/V30. We thank Dr. Uwe Pischel for helpful discussions.

■ REFERENCES

(1) (a) Findlater, M.; Choi, J.; Goldman, A. S.; Brookhart, M. In *Alkane C-H Activation by Single-Site Metal Catalysis*; Pérez, P. J., Ed.; Springer: Dordrecht, 2012; Chapter 4. (b) Haibach, M. C.; Kundu, S.; Brookhart, M.; Goldman, A. S. *Acc. Chem. Res.* **2012**, *45*, 947−958. (c) Choi, J.; MacArthur, A. H. R.; Brookhart, M.; Goldman, A. S. *Chem. Rev.* **2011**, *111*, 1761−1779.

(2) Caspary1, K. J.; Gehrke, H.; Heinritz-Adrian, M.; Schwefer, M. In *Handbook of Heterogeneous Catalysis*; Ertl, G., Knözinger, H., Schütz, F., Weitkamp, F., Eds.; Wiley: Weinheim, 2008.

(3) (a) Feiters, M. C.; Rowan, A. E.; Nolte, R. J. M. *Chem. Soc. Rev.* **2000**, *29*, 375−384. (b) Costas, M.; Mehn, M. P.; Jensen, M. P.; Que, L., Jr. *Chem. Rev.* **2004**, *104*, 939−986. (c) Hirao, H.; Kumar, D.; Que, L., Jr.; Shaik, S. *J. Am. Chem. Soc.* **2006**, *128*, 8590−8606. (d) Que, L., Jr. *Acc. Chem. Res.* **2007**, *40*, 493−500. (e) Nam, W. *Acc. Chem. Res.* **2007**, *40*, 522−531. (f) Murahashi, S. I.; Zhang, D. *Chem. Soc. Rev.* **2008**, *37*, 1490−1501. (g) Bell, C. B.; Wong, S. D.; Xiao, Y. M.; Klinker, E. J.; Tenderholt, A. L.; Smith, M. C.; Rohde, J. U.; Que, L., Jr.; Cramer, S. P.; Solomon, E. I. *Angew. Chem., Int. Ed.* **2008**, *47*, 9071−9074. (h) Bell, S. R.; Groves, J. T. *J. Am. Chem. Soc.* **2009**, *131*, 9640−9641. (i) Pan, Z.; Wang, Q.; Sheng, X.; Horner, J. H.; Newcomb, M. *J. Am. Chem. Soc.* **2009**, *131*, 2621−2628. (j) Martinho, M.; Xue, G.; Fiedler, A. T.; Que, L., Jr.; Bominaar, E. L.; Münck, E. *J. Am. Chem. Soc.* **2009**, *131*, 5823−5830.

(4) (a) Kim, C.; Dong, Y.; Que, L., Jr. *J. Am. Chem. Soc.* **1997**, *119*, 3635−3636. (b) Company, A.; Prat, I.; Frisch, J. R.; Mas Balleste, R.; Güell, M.; Juhász, G.; Ribas, X.; Münck, E.; Luis, J. M.; Que, L., Jr.; Costas, M. *Chem.—Eur. J.* **2011**, *17*, 1622−1634. (c) Mukherjee, A.; Martinho, M.; Bominaar, E. L.; Münck, E.; Que, L., Jr. *Angew. Chem., Int. Ed.* **2009**, *48*, 1780−1783.

(5) (a) Balcells, D.; Raynaud, C.; Crabtree, R. H.; Eisenstein, O. *Chem. Commun.* **2009**, 1772−1774. (b) Hull, J. F.; Balcells, D.; Sauer, E. L. O.; Raynaud, C.; Brudvig, G. W.; Crabtree, R. H.; Eisenstein, O. *J. Am. Chem. Soc.* **2010**, *132*, 7605−7616.

(6) Shi, S.; Wang, Y.; Xu, A.; Wang, H.; Zhu, D.; Roy, S. B.; Jackson, T. A.; Busch, D. H.; Yin, G. *Angew. Chem., Int. Ed.* **2011**, *50*, 7321−7324.

(7) Luo, Y.-R. In *Comprehensive Handbook of Chemical Bond Energies*; CRC Press: Boca Ratón, FL, 2007.

(8) Cho, K.-B.; Wu, X.; Lee, Y.-M.; Kwon, Y.-H.; Shaik, S.; Nam, W. *J. Am. Chem. Soc.* **2012**, *133*, 20222−20225.

(9) (a) Wender, I. *Fuel Process. Technol.* **1996**, *48*, 189−297. (b) Molinari, R.; Poeria, T. *Asia-Pac. J. Chem. Eng.* **2010**, *5*, 191−206.

(10) (a) Trofimenko, S. In *Scorpionates: The Coordination Chemistry of Polypyrazolylborate Ligands*; Imperial College Press: London, 1999. (b) Pettinari, C. *Scorpionates II: Chelating Borate Ligands*; Imperial College Press: River Edge, NJ, 2008.

(11) Conde, A.; Díaz-Requejo, M. M.; Pérez, P. J. *Chem. Commun.* **2011**, *47*, 8154−8156.

(12) (a) Barton, D. H. R.; Béviére, S. D.; Chavarisi, W.; Csuhai, E.; Doller, D. *Tetrahedron* **1992**, *48*, 2895−2910. (b) Velusamy, S.; Punniyamurthy, T. *Tetrahedron Lett.* **2003**, *44*, 8955−8957. (c) Kirillov, A. M.; Kopylovich, M. N.; Kirillova, M. V.; Haukka, M.; Guedes da Silva, M. F. C.; Pombeiro, A. J. L. *Angew. Chem., Int. Ed.* **2005**, *44*, 4345−4349. (d) Kirillov, A. M.; Kopylovich, M. N.; Kirillova, M. V.; Karabach, E. Y.; Haukka, M.; Guedes da Silva, M. F. C.; Pombeiro, A. J. L. *Adv. Synth. Catal.* **2006**, *348*, 159−174. (e) Silva, T. F. S.; Alegria, E. C. B. A.; Martins, L. M. D. R. S.; Pombeiro, A. J. L. *Adv. Synth. Catal.* **2008**, *350*, 706−716. (f) Mirkhani, V.; Moghadam, M.; Tangestaninejad, S.; Mohammadpoor-Blatork, I.; Rasouli, N. *Catal. Commun.* **2008**, *9*, 2411−2416. (g) Detoni, C.; Carvalho, N. M. F.; Aranda, D. A. G.; Louis, B.; Antunes, O. A. C. *Appl. Catal., A* **2009**, *365*, 281−286. (h) Mahmudov, K. T.; Kopylovich, M. N.; Guedes da Silva, M. F. C.; Figiel, P. J.; Karabach, Y. Y.; Pombeiro, A. J. L. *J. Mol. Catal. A: Chem.* **2010**, *318*, 44−50. (i) Kopylovich, M. N.; Mahmudov, K. T.; Guedes da Silva, M. F. C.; Figiel, P. J.; Karabach, Y. Y.; Kuznetsov, M. L.; Luzyanin, K. V.; Pombeiro, A. J. L. *Inorg. Chem.* **2011**, *50*, 918−931. (j) Fernandes, R. R.; Lasri, J.; Guedes da Silva, M. F. C.; da Silva, J. A. L.; Fraústo da Silva, J. J. R.; Pombeiro, A. J. L. *Appl.*

Catal., A **2011**, *402*, 110−120. (k) Goberna-Ferrón, S.; Lillo, V.; Galán-Mascarós, J. R. *Catal. Commun.* **2012**, *23*, 30−33.
(13) For one example of hexane hydroxylation see: Barton, D. H. R.; Csuhai, E.; Doller, D.; Geletii, Y. V. *Tetrahedron* **1991**, *47*, 6561−6570.
(14) See for example: Atkins, P.; Overton, T.; Rourke, J.; Weller, M.; Armstrong, F. In *Inorganic Chemistry*, 4th ed.; Oxford University Press: Oxford, 2006; Chapter 15.
(15) Walling, C.; Johnson, R. A. *J. Am. Chem. Soc.* **1975**, *97*, 363−367.
(16) (a) Kirillova, M. V.; Kirillov, A. M.; Guedes da Silva, M. F. C.; Pombeiro, A. J. L. *Eur. J. Inorg. Chem.* **2008**, 3423−3427. (b) Shulpin, G. B. *J. Mol. Catal. A: Chem.* **2002**, *189*, 39−66.
(17) Lyons, J. E.; Ellis, P. E.; Myers, H. K., Jr. *J. Catal.* **1995**, *155*, 59−73.
(18) (a) Sawyer, D. T.; Kang, C.; Llobet, A.; Redman, C. *J. Am. Chem. Soc.* **1993**, *115*, 5817−5817. (b) Hagem, J. P.; Llobet, A.; Sawyer, D. T. *Bioorg. Med. Chem.* **1995**, *3*, 1383−1388.
(19) (a) Bossmann, S. H.; Oliveros, E.; Göb, S.; Siegwart, S.; Dahlen, E. P.; Payawan, Jr.; Straub, M.; Wörner, M.; Braun, A. M. *J. Phys. Chem. A* **1998**, *102*, 5542−5550. (b) Marusawa, H.; Ichikawa, K.; Narita, N.; Murakami, H.; Ito, K.; Tezuka, T. *Bioorg. Med. Chem.* **2002**, *10*, 2283−2290.
(20) For the generation of metal-oxo species using oxone see: Chow, T. W.-S.; Liu, Y.; Che, C.-M. *Chem Commun.* **2011**, *47*, 11204−11206 and references cited therein.
(21) Mahy, J.-P.; Bedy, G.; Battioni, P.; Mansuy, D. *New J. Chem.* **1989**, *13*, 651−657.
(22) Balcells, D.; Clot, E.; Eisenstein, O. *Chem. Rev.* **2010**, *110*, 749−823.
(23) (a) Hay-Motherwell, R. S.; Wilkinson, G.; Hussain-Bates, B.; Hursthouse, M. B. *Polyhedron* **1993**, *12*, 2009−2012. (b) Jin, N.; Ibrahim, M.; Spiro, T. G.; Groves, J. T. *J. Am. Chem. Soc.* **2007**, *129*, 12416−12417. (c) Li, F.; Meier, K. K.; Cranswick, M. A.; Chakrabarti, M.; Van Heuvelen, K. M.; Münck, E.; Que, L. *J. Am. Chem. Soc.* **2011**, *133*, 7256−7259. (d) Prat, I.; Mathieson, J. S.; Güell, M.; Ribas, X.; Luis, J. M.; Cronin, L.; Costas, M. *Nat. Chem.* **2011**, *3*, 788−793.
(24) (a) Yoshizawa, K.; Kihara, N.; Kamachi, T.; Shiota, Y. *Inorg. Chem.* **2006**, *45*, 3034−3041. (b) Crespo, A.; Marti, M. A.; Roitberg, A. E.; Amzel, L. M.; Estrin, D. A. *J. Am. Chem. Soc.* **2006**, *128*, 12817−12828. (c) Huber, S. M.; Ertem, M. Z.; Aquilante, F.; Gagliardi, L.; Tolman, W. B.; Cramer, C. J. *Chem.—Eur. J.* **2009**, *15*, 4886−4895. (d) Poater, A.; Ribas, X.; Llobet, A.; Cavallo, L.; Solà, M. *J. Am. Chem. Soc.* **2008**, *130*, 17710−17717. (e) Güell, M.; Luis, J. M.; Siegbahn, P. E. M.; Solà, M. *J. Biol. Inorg. Chem.* **2009**, *14*, 273−285. (f) Itoh, S.; Taki, M.; Nakao, H.; Holland, P. L.; Tolman, W. B.; Que, L.; Fukuzumi, S. *Angew. Chem., Int. Ed.* **2000**, *39*, 398−400. (g) García-Bosch, I.; Ribas, X.; Costas, M. *Chem.—Eur. J.* **2012**, *18*, 2113−2122.
(25) García-Bosch, I.; Company, A.; Cady, C. W.; Styring, S.; Browne, W. R.; Ribas, X.; Costas, M. *Angew. Chem., Int. Ed.* **2011**, *50*, 5648−5653.
(26) (a) Lundberg, M.; Blomberg, M. R. A.; Siegbahn, P. E. M. *Inorg. Chem.* **2004**, *43*, 264−274. (b) Siegbahn, P. E. M.; Crabtree, R. H. *J. Am. Chem. Soc.* **1999**, *121*, 117−127.
(27) Balcells, D.; Raynaud, C.; Crabtree, R. H.; Eisenstein, O. *Chem. Commun.* **2008**, 744−746.
(28) (a) Groves, J. T. *J. Chem. Educ.* **1985**, *62*, 928−931. (b) Groves, J. T.; McClusky, G. A. *J. Am. Chem. Soc.* **1976**, *98*, 859−861.
(29) (a) Harvey, J. N.; Aschi, M.; Schwarz, H.; Koch, W. *Theor. Chem. Acc.* **1998**, *99*, 95−99. (b) Poli, R.; Harvey, J. N. *Chem. Soc. Rev.* **2003**, *32*, 1−8. (c) Manner, V. W.; Lindsay, A. D.; Mader, E. A.; Harvey, J. N.; Mayer, J. M. *Chem. Sci.* **2012**, *3*, 230−243.
(30) (a) Meunier, B.; de Visser, S. P.; Shaik, S. *Chem. Rev.* **2004**, *104*, 3947−3980. (b) Shaik, S.; Cohen, S.; Wang, Y.; Chen, H.; Kumar, D.; Thiel, W. *Chem. Rev.* **2010**, *110*, 949−1017.
(31) Donoghue, P. J.; Tehranchi, J.; Cramer, C. J.; Sarangi, R.; Solomon, E. I.; Tolman, W. B. *J. Am. Chem. Soc.* **2011**, *133*, 17602−17605.
(32) Usharani, D.; Janardanan, D.; Shaik, S. *J. Am. Chem. Soc.* **2011**, *133*, 176−179.
(33) Barnett, S. M.; Goldberg, K. I.; Mayer, J. M. *Nat. Chem.* **2012**, *4*, 498−502.
(34) (a) Mealli, C.; Arcus, C. S.; Wilkinson, J. L.; Marks, T. J.; Ibers, J. A. *J. Am. Chem. Soc.* **1976**, *98*, 711−718. (b) Schneider, J. L.; Carrier, S. M. C.; Ruggiero, E.; Young, V. G., Jr.; Tolman, W. B. *J. Am. Chem. Soc.* **1998**, *120*, 11408−11418. (c) Mairena, M. A.; Urbano, J.; Carbajo, J.; Maraver, J. J.; Alvarez, E.; Díaz-Requejo, M. M.; Pérez, P. J. *Inorg. Chem.* **2007**, *46*, 7428−7435.
(35) Frisch, M. J. et al. *Gaussian 09*, Revision A.02; Gaussian, Inc.: Wallingford, CT, 2009.
(36) (a) Becke, A. D. *Phys. Rev. A* **1988**, *38*, 3098−3100. (b) Lee, C.; Yang, W.; Parr, R. G. *Phys. Rev. B* **1988**, *37*, 785−789. (c) Miehlich, B.; Savin, A.; Stoll, H.; Preuss, H. *Chem. Phys. Lett.* **1989**, *157*, 200−206.
(37) (a) Hehre, W. J.; Ditchfield, R.; Pople, J. A. *J. Chem. Phys.* **1972**, *56*, 2257−2261. (b) Ehlers, A. W.; Böhme, M.; Dapprich, S.; Gobbi, A.; Höllwarth, A.; Jonas, V.; Köhler, K. F.; Stegmann, R.; Veldkamp, A.; Frenking, G. *Chem. Phys. Lett.* **1993**, *208*, 111−114. (c) Höllwarth, A.; Böhme, H.; Dapprich, S.; Ehlers, A. W.; Gobbi, A.; Jonas, V.; Köhler, K. F.; Stegmann, R.; Veldkamp, A.; Frenking, G. *Chem. Phys. Lett.* **1993**, *208*, 237−240. (d) Hariharan, P. C.; Pople, J. A. *Theor. Chim. Acta* **1973**, *28*, 213−222.
(38) (a) Andrae, D.; Häussermann, U.; Dolg, M.; Stoll, H.; Preuss, H. *Theor. Chim. Acta* **1990**, *77*, 123−141. (b) Bergner, A.; Dolg, M.; Küchle, W.; Stoll, H.; Preuss, H. *Mol. Phys.* **1993**, *80*, 1431−1441.
(39) (a) McLean, A. D.; Chandler, G. S. *J. Chem. Phys.* **1980**, *72*, 5639−5648. (b) Raghavachari, K.; Binkley, J. S.; Seeger, R.; Pople, J. A. *J. Chem. Phys.* **1980**, *72*, 650−654.
(40) (a) Hratchian, H. P.; Schlegel, H. B. *J. Chem. Phys.* **2004**, *120*, 9918−9924. (b) Hratchian, H. P.; Schlegel, H. B. *J. Chem. Theory Comput.* **2005**, *1*, 61−69.
(41) Barone, V.; Cossi, M. *J. Phys. Chem. A* **1998**, *102*, 1995−2001.
(42) (a) Balcells, D.; Ujaque, G.; Fernandez, I.; Khiar, N.; Maseras, F. *J. Org. Chem.* **2006**, *71*, 6388−6396. (b) Braga, A. A. C.; Ujaque, G.; Maseras, F. *Organometallics* **2006**, *25*, 3647−3658.
(43) (a) Poater, J.; Solà, M.; Rimola, A.; Rodríguez-Santiago, L.; Sodupe, M. *J. Phys. Chem. A* **2004**, *108*, 6072−6078. (b) Rios-Font, R.; Sodupe, M.; Rodríguez-Santiago, L.; Taylor, P. R. *J. Phys. Chem. A* **2010**, *114*, 10857−10863.
(44) (a) Purvis, G. D., III; Bartlett, R. J. *J. Chem. Phys.* **1982**, *76*, 1910−1918. (b) Scuseria, G. E.; Janssen, C. L.; Schaefer, H. F., III. *J. Chem. Phys.* **1988**, *89*, 7382−7387. (c) Pople, J. A.; Head-Gordon, M.; Raghavachari, K. *J. Chem. Phys.* **1987**, *87*, 5968−5975.
(45) Zhao, Y.; Truhlar, D. G. *J. Phys. Chem. A* **2004**, *108*, 6908−6918.
(46) Zhao, Y.; Truhlar, D. G. *Theor. Chem. Acc.* **2008**, *120*, 215−241.
(47) Reed, A. E.; Curtiss, L. A.; Weinhold, F. *Chem. Rev.* **1988**, *88*, 899−926.